Title

Impacts of enhanced microbial-photoreductive and suppressed dark microbial reductive dissolution on the mobility of As and Fe in flooded tailing soils with zinc sulfide

Authors

Chen, Zheng
Dong, Guowen
Chen, Yibin
et al.

Publication Date

2019-09-01

DOI

10.1016/j.cej.2019.04.130

Peer reviewed

Chemical Engineering Journal 372 (2019) 118–128

Contents lists available at ScienceDirect

Chemical Engineering Journal

journal homepage: www.elsevier.com/locate/cej

Impacts of enhanced microbial-photoreductive and suppressed dark microbial reductive dissolution on the mobility of As and Fe in flooded tailing soils with zinc sulfide

Zheng Chen[a,e,*], Guowen Dong[c,d], Yibin Chen[b], Honghui Wang[e], Shurui Liu[c], Zhijie Chen[e], Chenghu Yang[a], Xu Shang[a], Randy Dahlgren[a,f]

[a] Zhejiang Provincial Key Laboratory of Watershed Science & Health, Wenzhou Medical University, Wenzhou 325035, People's Republic of China
[b] Key Laboratory of Measurement & Control System for Coastal Environment, Fuqing Branch of Fujian Normal University, Fuqing 350300, People's Republic of China
[c] Department of Chemical & Biochemical Engineering, College of Chemistry & Chemical Engineering, Xiamen University, Xiamen 361001, People's Republic of China
[d] College of Resources and Chemical Engineering, Sanming University, Sanming 365004, People's Republic of China
[e] Department of Environmental Science, School of Environmental Science & Engineering, Tan Kah Kee College, Xiamen University, Zhangzhou 363105, People's Republic of China
[f] Department of Land, Air and Water Resources, University of California, Davis, Davis, CA 95616, United States

HIGHLIGHTS

- Microbial-photoelectrochemical synergetic process favors As(V)/Fe(III) reduction.
- Mineral photoelectrons can participate in microbial electron transfer chains.
- Suppressed As(V)/Fe(III) reduction is exhibited in ZnS-amended soil under dark.
- Biogeochemical cycles of metal in sunlight-enriched soils deserve more attention.

GRAPHICAL ABSTRACT

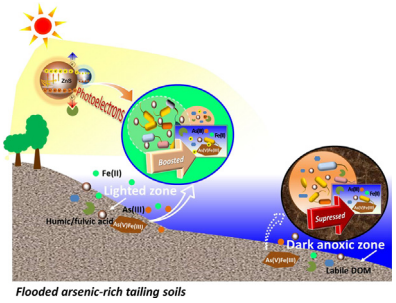

ARTICLE INFO

Keywords:
Zinc sulfide
Iron
Arsenic
Photoelectrons
Microbe
Tailing soils

ABSTRACT

Semiconducting minerals are ubiquitous in soil and their association with microbes often affects the environment. In this study, the impacts of zinc sulfide (ZnS, used as a model compound for semiconducting sphalerite) on As/Fe mobility of flooded tailing soils under dark and intermittent illumination conditions were elucidated for the first time. Microbial reductive dissolution of As(V) and Fe(III) was more pronounced under intermittent illumination than under dark conditions. In ZnS-amended soils, release of As(III) and Fe(II) was 1.3 and 1.7 times higher, respectively, under intermittent illumination than the highest concentrations released from soils amended with acetate alone under dark conditions (12741.1 ± 714.3 μg/L and 37.9 ± 2.3 mg/L, respectively). However, under dark conditions in ZnS-amended soil, the release of As(III) and Fe(II) was 0.8 and 0.7 times that of the highest concentrations released from soils amended with acetate under dark conditions, respectively. Treatment with ZnS potentially decreased the abundance of several metal-reducing bacteria (e.g., *Bacillus*, *Geobacter*, *Clostridium*, and *Desulfitobacterium*), which resulted in lower As/Fe reduction than for the acetate alone treatment under dark conditions. However, under intermittent illumination, the excited mineral photoholes were scavenged by humic/fulvic acids, and photoelectrons were synchronously separated and participated

* Corresponding author at: Zhejiang Provincial Key Laboratory of Watershed Science and Health, School of Public Health and Management, Wenzhou Medical University, Wenzhou 325035, People's Republic of China.
E-mail address: chenzheng_new@163.com (Z. Chen).

https://doi.org/10.1016/j.cej.2019.04.130
Received 16 February 2019; Received in revised form 9 April 2019; Accepted 19 April 2019
Available online 20 April 2019

in the microbial electron chain. The fortification provided by the photoelectrons subsequently boosted As/Fe reduction, even though there was a lower abundance of metal-reducing bacteria. Hence, this study provides an in-depth understanding of the impacts of semiconducting minerals on the fates of metal pollutants, microbial diversity, and the bioavailability of dissolved organic matter in flooded soils.

1. Introduction

Arsenic-bearing slag from mine tailing sites is a prominent environmental hazard and often results in adverse environmental impacts, such as land degradation and toxicological effects to crop growth and local residents [1,2]. The pattern of arsenic (As) in soil is closely correlated with the enrichment of iron (Fe) through the formation of As-Fe-bearing minerals (such as arsenoferrite) by co-precipitation [3,4]. Our previous studies demonstrated that microbial reductive dissolution of Fe(III)-bearing (hydr)oxides largely determined the transport and fate of As under anaerobic-reducing conditions, and resulted in elevated release of As from flooded soils [5,6]. The elucidated mechanism involved a metal-reducing bacteria-driven extracellular electron transfer (EET) process. This process can be accelerated by metal-reducing bacteria through synchronous oxidation of extracellular electron donors (such as labile dissolved organic matter (DOM)) and utilization of minerals with high valence states for energy conversion in the presence of redox mediators (such as biochar and quinone compounds) [7,8]. Therefore, the underlying electrical interplay pattern between metal-reducing bacteria and As-Fe-bearing minerals in tailing soils is related to the fate and transport of As/Fe, as well as the bioavailability of DOM.

The abundant semiconducting minerals in natural sediments and soils, such as hematite, goethite, and rutile, are highly responsive to sunlight [7,9]. Upon illumination, mineral photoelectrons are excited from their valence band to the conduction band of semiconducting minerals, forming photoelectron-hole pairs and triggering a series of redox reactions [10]. The separation of photoelectron-hole pairs and the released energy are desirable for non-photosynthetic microorganisms [11]. This suggests that possible synergetic interactions between mineral photoelectrons, semiconducting minerals, and microorganisms occur when there is a lack of bioavailable electron donors, and the excited photoelectrons are transferred to metal-reducing bacteria for metabolism [12,13]. In recent years, photocatalysis driven by semiconducting materials has received considerable attention as it may be used in solar energy conversion and environmental remediation [14–16]. However, the impact of the semiconducting mineral-driven biogeochemical processes of metal pollutants in soil under sunlight illumination has not been systematically examined. Such information may reveal the presence of a hybrid microbial-photoelectrochemical system involved in solar-to-electrical conversion for metal-reducing bacteria that regulate As/Fe mobility in organic matter limited soils.

Sphalerite (cubic β-zinc sulfide structure) is a representative semiconducting metal-sulfide mineral that is highly responsive to solar irradiation at the Earth's surface [17]. Owing to the favorable negative potential of the conduction band of sphalerite (-1.4 V vs. SCE) [18], there are many amendments that can favor the photocatalytic reductive degradation of organic pollutants, such as the photoreductive degradation of carbon tetrachloride and decolorization of azo dye by sphalerite [19,20]. Considering the widespread presence of natural sphalerite in the Earth's surface, it is reasonable to infer that sphalerite could regulate the fate of As/Fe, organic carbon stability in soil, and diversity of the microbial community through delivering solar energy to the indigenous metal-reducing bacteria and As-Fe-bearing minerals in soils. Nevertheless, until now, few studies have examined the impact of sphalerite on the fate of As/Fe in arsenic-rich soils, particularly in those receiving mine tailings. Hence, there is an important need for research targeting the sphalerite-driven microbial-photoelectrochemical pathway responsible for the fate and transport of As/Fe.

In this study, we selected zinc sulfide (ZnS) as a model compound of sphalerite to examine its impact on the fate of As/Fe in flooded tailing soils. The specific objectives of this paper are to (i) compare the speciation and mobilization performance of As/Fe in ZnS-amended soils with and without light illumination, and (ii) determine the connection between diversity of the microbial community and DOM modification linked to the fate of As/Fe in flooded tailing soils. The findings of this study will provide a newly identified a new electron transfer pathway between metal-reducing bacteria and semiconducting minerals that might be a vital component of biogeochemical metal cycles.

2. Methods and materials

2.1. Soil sampling

Arsenic-rich soils were sampled from a realgar tailing mine near Heshan Village, Shimen County in Changde City, central China. Detailed characteristics of the sampling site were previously described by Dong et al. [21]. Soil samples were collected from a low-lying land area on abandoned cropland. A soil corer (20 × 20 cm square, 10 cm in height) was used to obtain soil cores from each sampling site (total depth of 20–30 cm). After sampling, the soils were uniformly mixed, combined to form a composite sample, sealed in a sterile plastic bag, and transported to the lab. Subsamples were naturally air-dried, sieved to < 2 mm, and soil properties analyzed as outlined in Method S1. Select chemical and mineralogical properties of the experimental soils are shown in Table S1. According to x-ray diffractogram (XRD) spectra of the soil minerals, the main oxidation states of Fe and As in the crystalline compounds of the arsenic-rich soils are Fe(III) and As(V) (Fig. S1). To retain the original environment for the survival of indigenous bacteria, moist subsamples of soil were stored at 4 °C in polyethylene vinyl containers [5].

2.2. Anaerobic soil microcosm incubation

To investigate the influence of ZnS on the mobilization and speciation of As and Fe from flooded tailing soils, batch anaerobic microcosm assays were conducted in triplicate using 50-mL serum bottles. ZnS powder (99.99% and 3.3–4.3 μm) was purchased from Aladdin Company (United States). UV–vis diffuse reflectance (DRS) and XRD spectra, and a SEM image of the ZnS are shown in Figs. S2 and S3. The intrinsic bandgap and maximum absorption wavelength of ZnS are 3.52 eV and 350 nm, respectively, which are close to those of natural sphalerite (3.60 eV and 345 nm) [17].

The experimental anaerobic soil microcosms contained 12.0 g soil, 36.0 mL of 30.0-mM sodium acetate (NaAc) solution, and 0.10 g ZnS. Two biotic amendments were designed as follows: (i) microcosms were incubated under intermittent illumination, and (ii) microcosms were incubated under dark conditions. Two biotic control assays that were not supplemented with ZnS were also prepared and incubated under the respective illumination conditions. Another batch of anaerobic abiotic microcosms was simultaneously incubated by amending sterile soils with sodium acetate in the absence or presence of sterile ZnS under parallel conditions. All samples were incubated at 30 °C. To maintain an anoxic environment, high-purity nitrogen gas was bubbled into the liquid phase for 60 min and the headspace for another 30 min before sealing the serum bottles. To simulate natural conditions with the alternation of day and night, the incubator (MGC-300A, Yiheng, China) was programmed to provide 12 h light and 12 h darkness per day. The simulated sunlight was supplied with white LED irradiation, with

approximate light energy of 50 μmol/m^2·s.

2.3. Bioelectrochemical reactor configuration and electrochemical measurements

To determine the electron transfer performance, the electrogenesis capacity was estimated in an air-cathode electrochemical reactor. A batch of commercially available water bottles (Fig. 1a and b) (348 mL, Baisuishan, Ganten Co., Ltd, China) was modified and configured as single-chamber electrochemical reactors (Fig. 1a) composed of an anode and cathode. Commercial carbon cloths (7 × 7 cm, CW1001, purchased from Taiwan Carbon Technology Co., Ltd, Taiwan) were used as the anode and connected to the circuit via titanium wires. Upon connecting the circuit, the electrodes that enabled the oxygen reduction reaction served as the cathode. Here, an air-cathode membrane electrode was assembled following a method proposed by *Wu* et al., with a slight modification [22]. To fabricate an assembled air-cathode, a rod-form polyvinyl alcohol-hydrogel elastomer membrane electrode was loaded into a modified 15.0-mL screw-top plastic centrifuge tube. Details of the construction and fabrication procedures for the assembled air-cathodes are presented in Fig. S4 and Method S2.

Control reactors were incubated with 75.0 g of anaerobic arsenic-enriched soils and 225.0 mL of 30.0-mM sodium acetate solution, while the experimental reactors were also supplemented with 0.625 g of ZnS powder. The deoxygenization procedures followed the N_2 gas purging mentioned above. In each branch circuit, an external resistance (1000 Ω) was connected between the anode and cathode to close the circuit. Thereafter, a chain of branch circuits was connected in parallel via an external circuit. Voltage across the resistance was recorded every 600 s by a multimeter (Keithley-2700, Tektronix, USA). All reactors were incubated and illuminated under the same incubation conditions used for the soil microcosms. The potential responses of all reactors were recorded to reflect the energy transfer performance of the corresponding systems.

Electrochemical behaviors in the electrochemical reactors were analyzed by measuring the cyclic voltammetry (CV) and electrochemical impedance spectroscopy (EIS) using an electrochemical analyzer (660D, CHI Instruments Inc. Shanghai, China) [15,23]. All measurements were taken from a standard three-electrode system with the defined filtrate as the electrolyte. The standard three-electrode system was composed of a Pt wire as the counter electrode, Ag/AgCl as the reference electrode, and a carbon cloth obtained from the corresponding amendment as the working electrode. The defined filtrate was obtained from the supernatant collected from the corresponding reactors and filtered through syringe filters (0.2 μm, nylon, Millipore, USA). CV analysis was conducted at a scan rate of 0.05 V/s over a potential window of −0.8 to 0.6 V for the experiments conducted in triplicate. To fit the EIS Nyquist plot, the potential bias was set at open circuit voltage with a frequency ranging from 100 kHz to 100 MHz and a scan amplitude of 5 mV [23].

2.4. Analytical methods

Concentrations of dissolved As(T) (total arsenic), As(III), Fe(T) (total iron), and Fe(II) were quantified at each temporal sampling point. Briefly, 5 mL of supernatant from each culture was passed through a sterile 0.45-μm nylon filter. The As(T) concentration was measured using an ICP-Mass Spectrometer (NexION 2000, PerkinElmer, USA) [6]. Dissolved As(III) was quantified through high-performance liquid chromatography coupled with hydride-generation atomic-fluorescence spectrometry (HPLC-AFS, Titan, SA-50, China) [24]. Dissolved Fe(II) and Fe(T) were measured using the ferrozine assay [2]. As the excited photo-holes could be scavenged by endogenous humic and/or fulvic acid-like compounds in the soil [25], the humic and fulvic acid-like compounds contained in the soil-extracted DOM were monitored using a fluorescence spectrophotometer (FS5, Edinburgh, UK). Humic and fulvic acid-like compounds were measured by determining their respective fluorescence intensities under emission wavelengths of 464 and 451 nm by fixing the excitation wavelength at 279 nm [26]. Prior to analysis, DOM was extracted from a mixture of 3.0 g of freeze-dried soil and 30.0 mL of Milli-Q water while stirring at 200 rpm for 24 h at 20 °C, which was then filtered through a 0.45-μm membrane filter (Millipore, USA) [27].

The dissolved organic carbon extracted from the liquid and soil phases (henceforth referred to as LDOC and SDOC) was measured using a TOC analyzer (Shimadzu, TOC-L CPH, Japan) to estimate the degradation of organic substrate that was associated with the supply of bio-electrons and photoelectrons. LDOC was determined from the supernatant of each microcosm, and SDOC was determined from the soil DOM filtrate of each microcosm. Soil DOM filtrate was extracted from a mixture of Milli-Q water and freeze-dried soil (10:1, volume/weight, shaken for 24 h with a mixing speed of 200 rpm at room temperature in the dark) [27]. Prior to determination of LDOC and SDOC, the supernatant and soil DOM filtrate were filtered through a 0.45 μm membrane filter (Millipore, USA). The content of SDOC (mg/g) was calculated using Eq. (1):

$$SDOC = \frac{C \times V}{m} \quad (1)$$

where C (mg/L) is the DOC concentration of the DOM filtrate, V (L) is

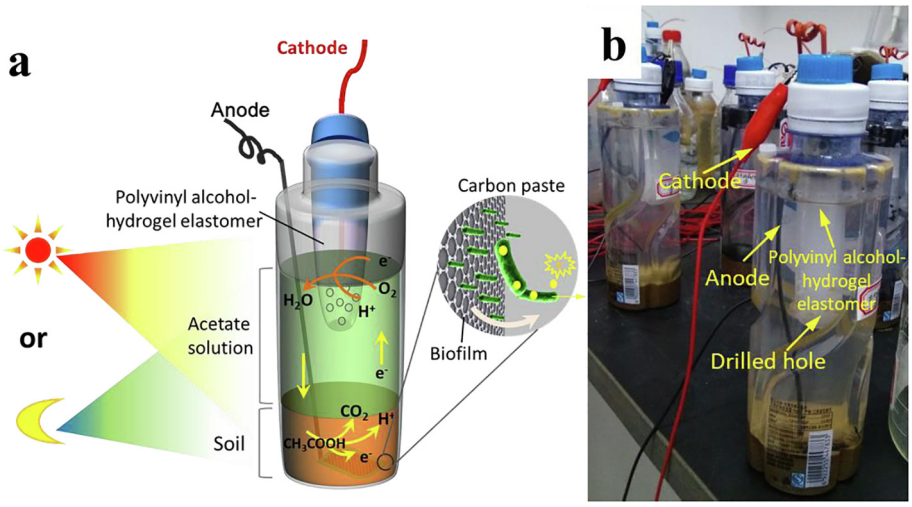

Fig. 1. Components of a new type of single-chamber microbial-photoelectrochemical reactor (a). Photograph of the single-chamber reactor used in this study (b).

volume of DOM filtrate, and m (g) is mass of freeze-dried soil. The ratio of absorbance at 250 nm to that at 365 nm (E_2/E_3) and the specific ultraviolet absorbance at 254 nm ($SUVA_{254}$) were used to estimate the moleculas size and aromatic degree of DOM [28]. Owing to the different ZnS-induced photodegradation capacities of the different organic substrates, the removal of TOC was monitored in the individual identification assays designated as: (1) ZnS (0.1 g) + sodium acetate solution (30 mM, 36 mL), and (2) ZnS (0.1 g) + soil extracted DOM solution (36 mL) under the same intermittent illumination.

2.5. Soil DNA extraction, PCR amplification, and sequencing

To explore changes in soil microbial composition in response to ZnS amendment and light illumination, DNA derived from the microcosms cultured for 7, 30, and 45 days was extracted and subjected to high-throughput sequencing targeting the V4-V5 regions of the bacterial 16S rRNA gene [29]. Total DNA was extracted from a 0.5-g soil sample using the Fast DNA Spin Kit for soil (MP Biomedical, USA). The 338F and 806R primers were used to amply the V4-V5 regions of the 16S rRNA gene by PCR, and the PCR products were pooled into 2% agarose gels for electrophoresis. The resulting products were purified using an AxyPrep DNA Gel Extraction Kit (Axygen Biosciences, USA) and quantified using QuantiFluor™ -ST Kit (Promega, USA). The purified amplicons were pooled at equal molar concentrations, and paired-end sequencing (2 × 250) was conducted on an Illumina MiSeq platform (Illumina, USA). The 16S rRNA gene sequence data were processed using the QIIME 1.8.0 tool kit. Details of the PCR amplification and sequencing analyses are reported in Method S3.

2.6. Data analysis

All data were analyzed using Microsoft Excel, Origin, and SPSS. Treatment effects were examined using analysis of variance (ANOVA). The least significant difference (LSD) multiple range test was conducted to determine the statistical significance ($P < 0.05$) between pairs using SPSS 22.0.

3. Results

3.1. Biotransformation of as and Fe

Fig. 2 presents the response of iron/arsenic mobilization to ZnS amendment under intermittent illumination and dark conditions. Throughout the incubation period, negligible concentrations (< 1.0 mg/L) of soluble Fe(T) and Fe(II) were released from the flooded sterile soils (Fig. 2a and b). In contrast, iron mobilization from the biotic assays was higher with the concentration of Fe(II) similar to that of Fe(T), indicating that microbial activity drove the reduction and mobilization of Fe(III). In addition, higher mobilization/reduction of Fe (III) was observed in soil under intermittent illumination compared to dark conditions. The addition of ZnS greatly increased mobilization/reduction of Fe(III) in the biotic assay under visible light illumination,

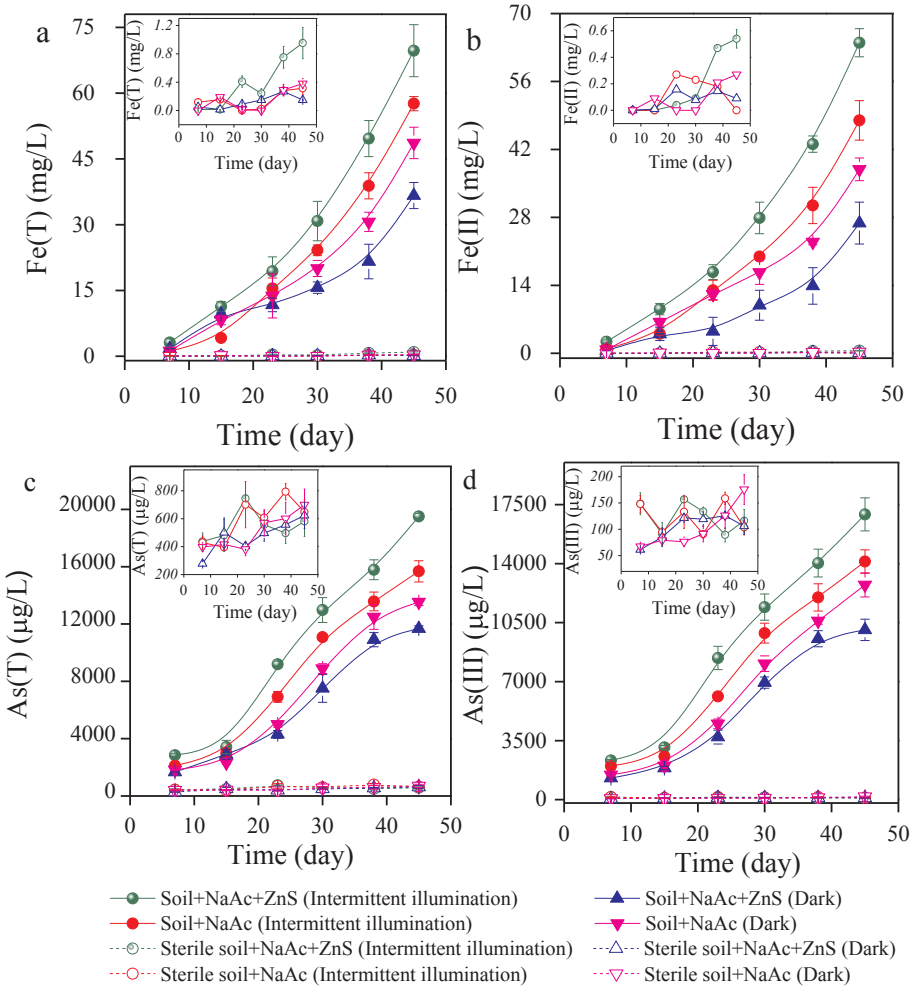

Fig. 2. Concentrations of soluble Fe(T) (a), Fe(II) (b), As(T) (c), and As(III) (d) released from the flooded tailing soils in response to intermittent illumination and dark conditions. Error bars represent the standard error for triplicate samples.

while an inhibitory effect was observed in the biotic assay without illumination. After 45 days of incubations, the highest Fe(II) concentrations in the presence and absence of ZnS for intermittent-illuminated soils were 64.0 ± 3.9 and 49.9 ± 4.1 mg/L, which were higher than those released from soils without illumination (26.8 ± 4.3 and 37.9 ± 2.3 mg/L).

The dissolution and reduction of As(V) followed a similar trend to that of Fe(III) under parallel conditions (Fig. 2c and d). Although appreciable amounts of As(T) were detected in the abiotic assays (280.3–740.5 μg/L), the reductive dissolution of As(V) was more prominent in the biotic assays, and released As(III) concentrations were much higher. In particular, the treatment with ZnS under intermittent illumination exhibited the highest release of As(III) from tailing soils with the highest As(III) concentration reaching 16924.1 ± 974.4 μg/L. Under dark conditions, the amount of As(III) released from the ZnS-supplemented soil was 0.79 times that of the control group (10072.3 ± 675.1 μg/L). Therefore, the gain or loss of electrons caused by ZnS amendment is likely correlated to the contribution of bio-electrons produced from microbial degradation of organic substrates, as well as photoelectrons excited from light-illuminated endogenous and/or exogenous semiconducting minerals [30,31].

3.2. Bioavailability of DOM

As labile DOM serves as an electron donor, a large amount of electrons obtained from the mineralization of labile DOM can be transferred from metal-reducing bacteria to electron donors (i.e., Fe(III) and As(V)) and form an integrated respiratory chain of EET [5,28]. As acetate was predominant in the liquid phase of the flooded soils, the removal of LDOC mainly resulted from the degradation of acetate. Throughout the incubation period, the removal of LDOC was lower in the intermittent-illuminated soils than from soils without illumination (Fig. 3a). After 45 days, almost 27.6%, 37.4%, 48.7%, and 59.10% of the LDOC was removed from the soils that were amended with acetate-ZnS (intermittent illumination), acetate alone (intermittent illumination), acetate-ZnS (dark), and acetate alone (dark), respectively. Loss of LDOC may be attributed to acetate used in the growth of soil microorganisms [32], microbially degraded for electron donation [6], or photodegraded by semiconducting minerals [33]. Considering the input-output electron balance in redox reactions, the behaviors for the conversion of organic substrates and electron transfer should be further studied.

Soils contain a wide array of organic substrates that play different roles in controlling electron transfer [5,25,32]. For instance, some low-molecular-weight DOM (such as sugars and amino acids) can readily serve as electron donors for soil microorganisms [32], while some heavy-molecular-weight DOM (such as fulvic and humic acids) can serve as scavengers of photoholes [25]. Thus, we monitored the removal of SDOC to further confirm the potential input of mineral photoelectrons in flooded soils. SDOC removal in all treatments contrasted with LDOC removal, i.e., higher removal of SDOC was observed in intermittent-illuminated soils than in soils without illumination (Fig. 3b). This suggested that the degradation of endogenous organic substrates was greater in intermittent-illuminated soils, and particularly in the intermittent-illuminated soils that were supplemented with ZnS. Moreover, DOM spectral results indicated that the ratio of E_2/E_3 and

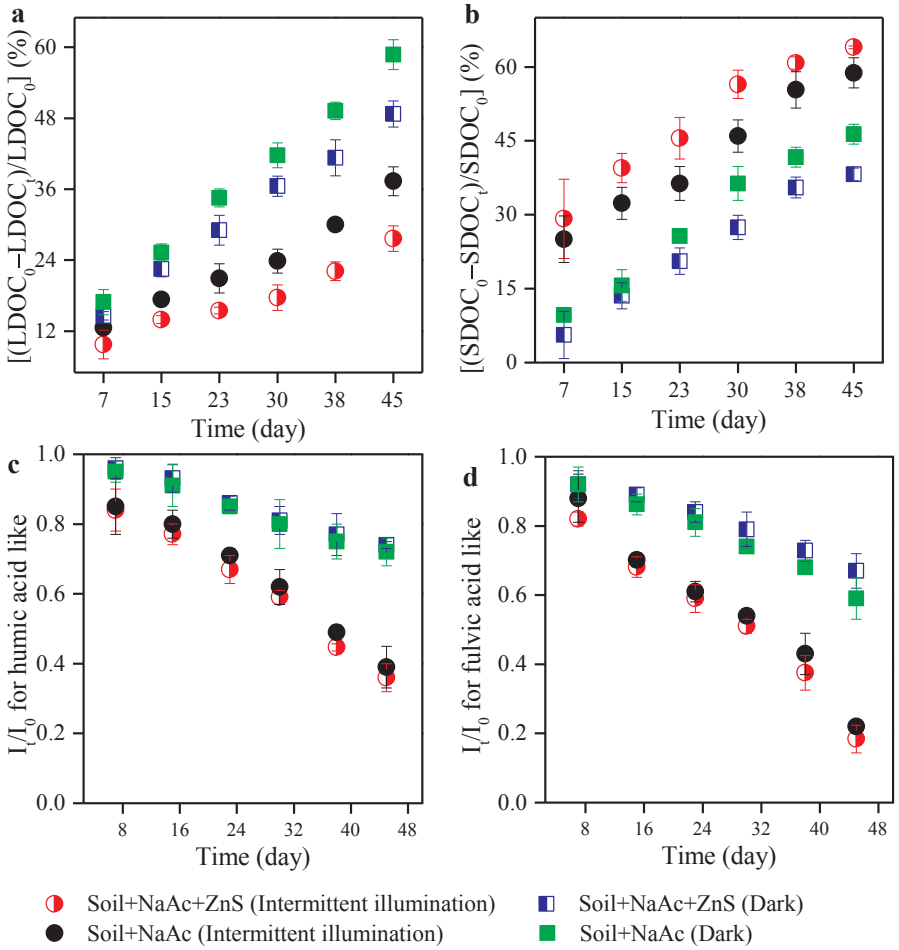

Fig. 3. Removal of LDOC (a) and SDOC (b) and dynamic changes in the fluorescence intensities of humic (c) and fulvic acid (d) in the respective amendments. (I_0 and I_t are the intensities of fluorescence emissions corresponding to initial conditions and each sampling time, respectively.).

$SUVA_{254}$, and fluorescence signals responding to fulvic and humic acid-like compounds were much lower in intermittent-illuminated soils than those in soils without illumination (Fig. 3c and d and Table S2). Therefore, it is likely that endogenous labile DOM in soils is photo-degraded and the photoelectrons are transferred to As(V)/Fe(III), while photoholes are quenched by the endogenous fulvic/humic acids in intermittent-illuminated soils.

3.3. Electron transfer performance

Fig. 4 presents the response of electron transfer performance to each amendment. The variation in the potential of the light illuminated reactors exhibited an instant photo-response under simulated sunlight illumination (Fig. 4a), as the potential increased with the light on and immediately decreased with the light off. In contrast, over 120.0 mV vs. Ag/AgCl of potential was retained in the ZnS-amended reactor under intermittent illumination, which was nearly 1.13-, 1.68-, and 3.10-times those in the intermittent-illuminated control reactor, dark control reactor, and ZnS-amended dark reactor, respectively (Fig. 4b). This demonstrates that ZnS amendment can excite more mineral photoelectrons under intermittent illumination.

Further, the CV curves presented in Fig. 4c indicate the characteristics of current generation derived from the biofilm matrix. For the protocol with supplementation with ZnS, the maximum current density was 10.56 mA/m^2 higher than the dark control reactor (9.43 mA/m^2) with intermittent illumination, but was 4.82 mA/m^2 lower without light illumination. This electrochemical performance could be a response to the reductive dissolution of As(V)/Fe(III) from soil to ZnS amendment and illuminated conditions (Fig. 2). As indicated by the smallest diameter of the curve, coincidentally, the reactor that was amended with ZnS and light illumination exhibited the lowest charge-transfer resistance among all electrochemical reactors (Fig. 4d). Hence, these electrochemical characteristics suggest that amendment with ZnS under illumination can boost photoelectron transfer, while the behavior of ZnS under dark conditions appeared to suppress electron transfer. As bio-electrons were supplied from microbial degradation of organic substrates [32,34], the composition of the microbial community should be further examined.

3.4. Composition of soil microbial community

High-throughput sequencing analysis was conducted to provide an overview of the composition of the active bacterial communities in the soil microcosms. In total, 14 distinct phyla were identified as predominant members of all biotic samples (Fig. S5). Generally, the phyla of *Firmicutes* (18–65%), *Proteobacteria* (17–36%), *Acidobacteria* (8–15%), *Bacteroidetes* (2–15%) and *Actinobacteria* (3–7%) were identified as the most dominant bacterial members under intermittent illumination and dark conditions. It appeared that the abundances of *Firmicutes* and *Acidobacteria* were increased under intermittent illumination, whereas the abundances of *Proteobacteria* and *Actinobacteria* were only increased under dark conditions. Specifically, the growth of *Proteobacteria* and *Acidobacteria* seemed to be inhibited by the presence of ZnS when compared to their respective control groups.

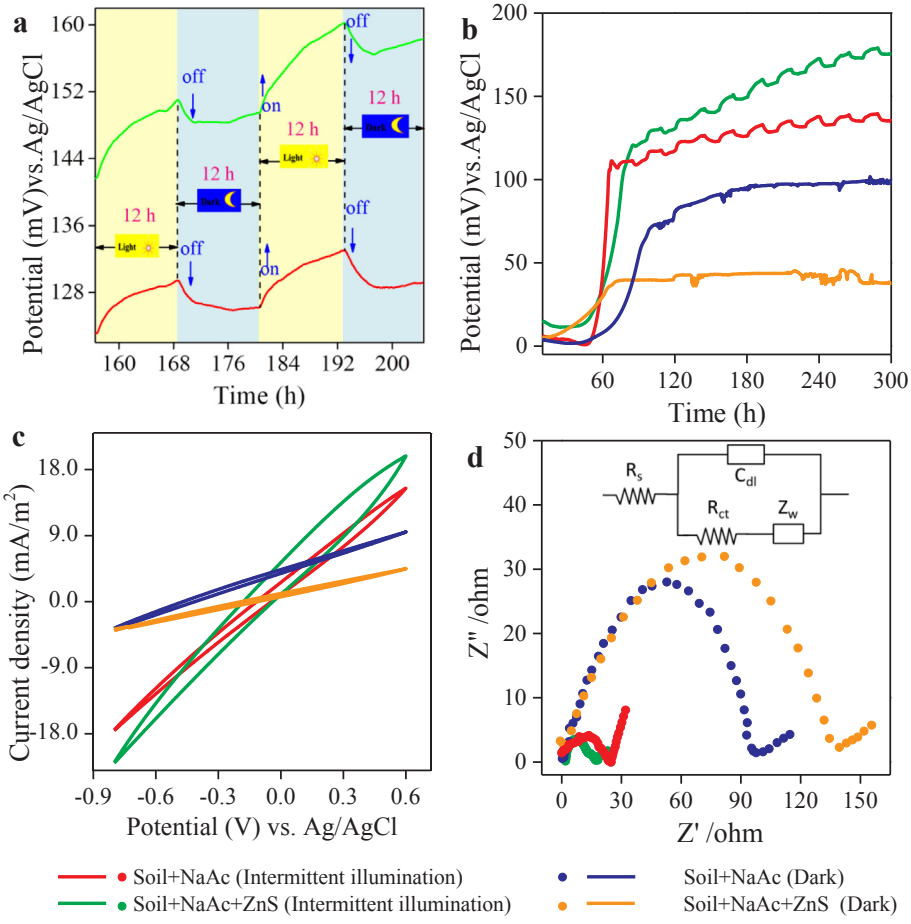

Fig. 4. Potential responses to illumination (a) and intermittent illumination and dark conditions (b) under an open circuit. Measurements of the CV curves (c) and electrochemical impedance spectra (d) to determine the electrochemical properties of the microbial-photoelectrochemical systems. In panel d, R_s, R_{ct}, Z_w, and C_{dl} are the ohmic resistance, electron-transfer resistance, Warburg impedance, and double layer capacitance, respectively.

Fig. 5 profiles the response of microbial diversity to each amendment at the genus level. *Bacillus*, *Geobacter*, and *Anaeromyxobacter* were representative metal-reducing bacteria [2,5,35], and were also the main genera in all biotic microcosms. Increases in the abundances of *Azotobacter* (2–11%), *Geobacter* (2–21%), and *Bacillus* (27–58%) under dark conditions were more pronounced than, or at least comparable to, those under intermittent illumination (1–5%, 3–8%, and 12–45%). These genera were dominant under darkness, indicating their specific roles and/or advantages in flooded ecosystems lacking illumination with sunlight. Additionally, ZnS addition resulted in a large increase in the abundance of *Bacillus* (38%) under the intermittently illuminated treatment at the end of the incubation period, while ZnS inhibited *Bacillus* in the dark treatment (27%). With the ZnS amendment, the abundance of *Geobacter* positively responded (8%) to intermittent illumination, but negatively responded (13%) to darkness, in contrast to their respective control groups (5% and 20%). Thus, ZnS addition under different illumination conditions resulted in different influences to the diversity of the soil microbial community and could affect the environment, to a certain extent [17,20].

4. Discussion

4.1. Soil microbial diversity response to ZnS amendment

Principal coordinate analysis (PCoA) revealed that the intermittent illumination treatments were similar, regardless of ZnS supplementation, but were distant from amendments with acetate-ZnS and acetate alone under dark conditions (Fig. 6a). Meanwhile, redundancy analysis (RDA) identified a positive relationship between environmental factors (including As(III), Fe(II), and SDOC) and representative metal-reducing bacteria (such as *Bacillus*, *Geobacter*, and *Anaeromyxobacter*) under intermittent illumination (Fig. 6b). This indicates that *Bacillus*, *Geobacter*, and *Anaeromyxobacter* species might be responsible for As/Fe reduction. However, in ZnS-amended soils under dark conditions, the abundance of *Anaeromyxobacter* did not correlate strongly with dissolved As (III) and Fe(II) concentrations ($r^2 = 0.578$, $P > 0.05$ and $r^2 = 0.300$, $P > 0.05$, respectively, Table 1). Therefore, the results suggest that these active microbes might regulate environmental effects through developing specific survival strategies (metal resistance or metabolic flexibility) under their respective conditions [36,37].

In this study, amendment with ZnS without illumination decreased the abundances of metal-reducing bacteria (Table 2). This may be explained by lower DOM bioavailability and lower As/Fe reduction in ZnS-amended soils than those in control samples under dark conditions (Figs. 2 and 3). In addition, we found intermittent illumination suppressed the enrichment of metal-reducing bacteria (Table 2), as indicated by the lower total abundances (33–34%) of metal-reducing bacteria than under dark conditions (48–61%). If EET occurred only through the acceptance of bio-electrons by metal-reducing bacteria, this might suggest restricted As/Fe reduction under a given environmental condition. We found that the magnitude of As/Fe reduction under intermittent illumination was greater than under dark conditions (Fig. 2) and was particularly magnified in the presence of ZnS. Reasons for enhanced As/Fe reduction include: (i) higher mineral photoelectron production under the illumination treatment [31,38], and (ii) stimulation by photodegradation of low-molecular-weight DOM by illumination, which then supplies electrons [39].

4.2. Degradation of DOM and separation and transfer of photoelectrons

If the supply of bio-electrons was the sole pathway for donating electrons, the lower degradation of labile DOM would not explain the higher As/Fe reduction in the intermittently illuminated soils. Therefore, some of the electrons may have originated from mineral photoelectrons [40,41], which then began a photoelectric conversion process to support As/Fe reduction. In addition to supplementation with the exogenous, superior semiconducting ZnS, the reductive dissolution of As(V)/Fe(III) in intermittent-illuminated soils was promoted by microbial-photoelectrochemical-coupled administration (Fig. 2). Moreover, the results of the identification assays indicated that the addition of ZnS induced a small amount of acetate photodegradation alongside the visible photodegradation of endogenous soil DOM (Fig. S6). Due to the sensitive optical properties of some labile DOM sources [42,43], some low-molecular-weight DOM might be easily photodegraded by oxidative photoholes under illumination conditions and thereafter supply more electrons. These results are further supported by the lower ratio of E_2/E_3 detected in the intermittently illuminated soils (Table S2). We infer that the greater amount of electrons in the intermittent-illuminated soils is likely supplied by mineral photoelectrons and photodegradation of endogenous low-molecular-weight DOM in

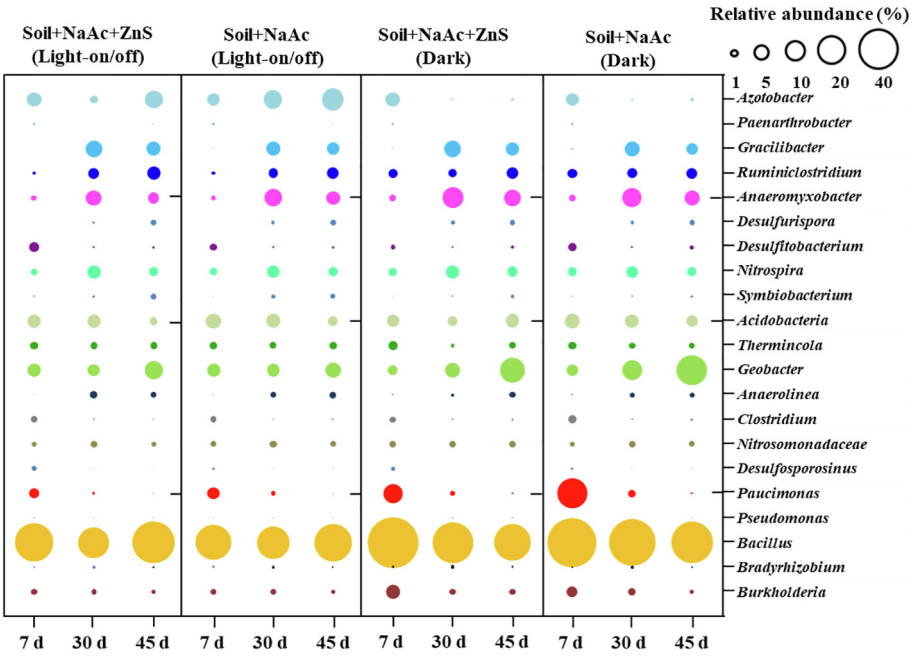

Fig. 5. Dynamic shift (7, 30, and 45 days) in the relative abundance of the potentially active bacterial community at the genus level in respective amendments.

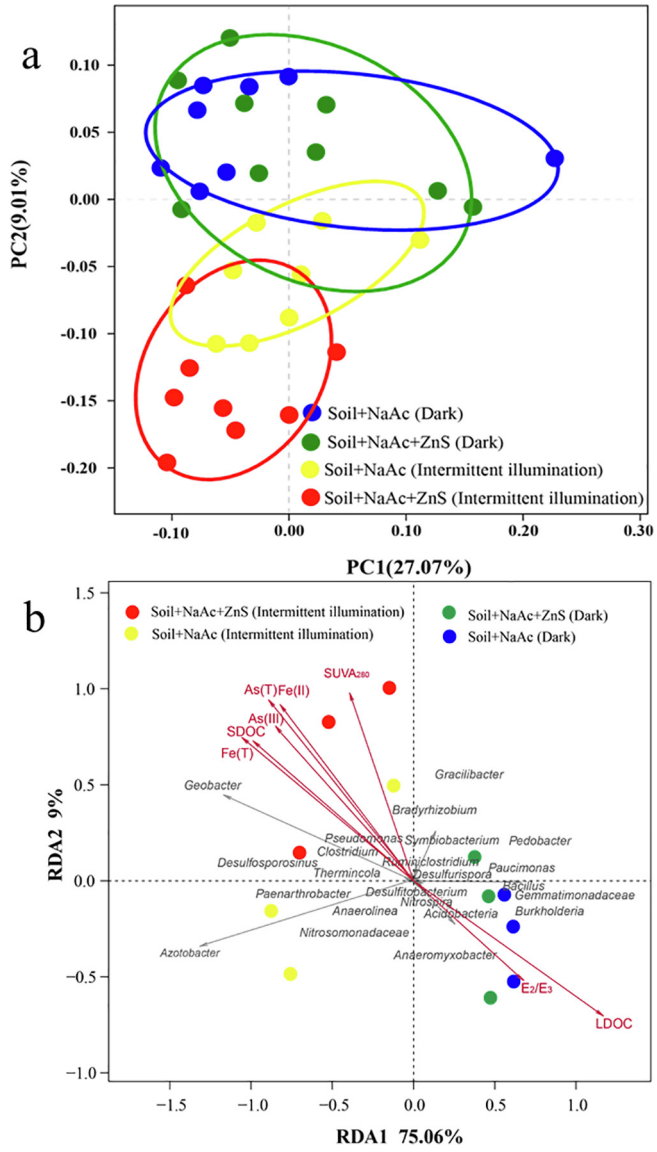

Fig. 6. Weighted UniFrac PCoA (a) of the soil microbial community based on 16S rRNA high-throughput sequencing, and RDA (b) based on environmental factors and microbial communities at the genus level.

flooded soils, in addition to microbial degradation of acetate.

The findings regarding DOM bioavailability (Figs. 3 and S6, and Table S2) provided further insight into the behavior of photoelectron transfer, and suggested that the recombination of electron-hole pairs under illumination was effectively suppressed. Further, the separation of electron-hole pairs was facilitated by the capture of the photohole by fulvic and/or humic acid [44–46]. In addition, sulfides in the soil are effective in scavenging the photohole [47]. These strategies might favor the transfer of photoelectrons from metal-reducing bacteria to As(V) and Fe(III), and effectively overcome the rapid recombination process. Thereafter, the synergy between microbial oxidation of organic matter and photodegradation of labile soil DOM, and enhanced photoelectrons transfer will further facilitate the reductive dissolution of As(V)/Fe(III) in flooded soils.

4.3. Electron transfer pathway associated with As/Fe mobilization

Results of this study indicated that interactions between semiconducting minerals and indigenous microorganisms boosted or inhibited As/Fe reduction, providing important information regarding the dissolution behavior of As in flooded tailing soils. Semiconducting ZnS appears to have an ecological and evolutionary disadvantage as it suppresses the enrichment of metal-reducing bacteria in flooded tailing soils under dark conditions (Fig. 7). The mechanism by which ZnS amendment inhibits the reductive dissolution of As(V)/Fe(III) from tailing soils under dark conditions is still unclear. As microbial activity plays an important role in controlling As/Fe mobility, the underlying mechanism might involve the expression of the targeted genes or complex redox protein systems for implementing electron transfer [48]. Therefore, suppression of metal-reducing *Bacillus* ($r^2 = -0.939$ and $P < 0.01$) and *Clostridium* ($r^2 = -0.890$ and $P < 0.01$) species by ZnS could be a reason for the inhibition of reductive dissolution of As(V) from tailing soils (Table 1).

In contrast, under illumination, mineral photoelectrons pass through the conductive band to soils, where they may indirectly transfer to metal-reducing bacteria and/or release As(V) and Fe(III) via reductive dissolution of As(V)/Fe(III) (illustrated in Fig. 7). Further, photogenerated holes in the valence band can mineralize low-molecular-weight compounds or be scavenged in the bulk phase (such as terrestrial humic substances or surface defect clusters) [44,49,50], facilitating the separation of photogenerated electron-hole pairs. Semiconducting minerals can also participate in microbial metabolism and may serve as an electron shuttle through employing photoholes as electron acceptors and mineral photoelectrons as electron donors in microbial electron transfer chains [31,38]. In the presence of semiconducting minerals and illumination, integration of semiconducting minerals with microbial biotransformation decouples the requirements for biocatalytic reaction and light-capture [49], creating a new pathway that boosts As/Fe mobilization in flooded soils via a hybrid microbial-photoelectrochemical conversion.

Table 1
Pearson correlation matrix for dissolved levels of As(III) and Fe(II) impacted by the abundances of key metal-reducing bacteria in respective amendments.

Correlation	Soil + NaAc + ZnS (Intermittent illumination)	Soil + NaAc (Intermittent illumination)	Soil + NaAc + ZnS (Dark)	Soil + NaAc (Dark)
Dissolved As(III)				
Bacillus	0.250 ($P = 0.550$)	0.195 ($P = 0.644$)	**−0.939** ($P < 0.01$)**	**−0.955** ($P < 0.01$)**
Geobacter	0.641 ($P = 0.087$)	0.559 ($P = 0.150$)	**0.821* ($P < 0.05$)**	**0.940** ($P < 0.01$)**
Anaeromyxobacter	0.420 ($P = 0.300$)	0.616 ($P = 0.104$)	0.578 ($P = 0.134$)	0.494 ($P = 0.213$)
Clostridium	**−0.897** ($P < 0.01$)**	**−0.906** ($P < 0.01$)**	**−0.890** ($P < 0.01$)**	**−0.818* ($P < 0.05$)**
Desulfitobacterium	**−0.891** ($P < 0.01$)**	**−0.841** ($P < 0.01$)**	−0.578 ($P = 0.134$)	−0.688 ($P = 0.059$)
Dissolved Fe(II)				
Bacillus	0.448 ($P = 0.266$)	0.341 ($P = 0.409$)	**−0.772* ($P < 0.05$)**	**−0.897** ($P < 0.01$)**
Geobacter	**0.790* ($P < 0.05$)**	**0.715* ($P < 0.05$)**	**0.884** ($P < 0.01$)**	**0.973** ($P < 0.01$)**
Anaeromyxobacter	0.198 ($P = 0.639$)	0.373 ($P = 0.363$)	0.300 ($P = 0.470$)	0.330 ($P = 0.425$)
Clostridium	**−0.761* ($P < 0.05$)**	**−0.751* ($P < 0.05$)**	−0.685 ($P = 0.061$)	−0.699 ($P = 0.054$)
Desulfitobacterium	**−0.752* ($P < 0.05$)**	−0.685 ($P = 0.061$)	−0.404 ($P = 0.321$)	−0.556 ($P = 0.153$)

Note: Symbols of * and ** are significant at levels 0.05 and 0.01 (2-tailed), respectively.

Table 2
The relative abundance (%) of representative metal-reducing bacteria at the genus level in respective amendments.

Amendments	Time	*Bacillus*	*Geobacter*	*Anaeromyxobacter*	*Clostridium*	*Desulfitobacterium*	Total
Soil + NaAc + ZnS (Intermittent illumination)	7 day	31.56 ± 3.35	3.86 ± 0.81	0.67 ± 0.12	1.03 ± 0.07	1.89 ± 0.55	39.01 ± 2.1
	30 day	22.06 ± 2.15	3.21 ± 0.47	5.89 ± 0.74	0.14 ± 0.02	0.12 ± 0.05	31.42 ± 5.6
	45 day	35.24 ± 4.71	5.90 ± 1.15	2.19 ± 0.16	0.04 ± 0.11	0.14 ± 0.06	43.51 ± 7.6
Soil + NaAc (Intermittent illumination)	7 day	26.40 ± 2.49	3.76 ± 0.52	0.41 ± 0.02	0.90 ± 0.21	1.10 ± 0.12	32.58 ± 8.4
	30 day	22.43 ± 3.64	3.45 ± 0.29	6.41 ± 0.45	0.13 ± 0.04	0.10 ± 0.01	32.43 ± 2.5
	45 day	29.42 ± 1.25	5.07 ± 1.15	5.65 ± 0.78	0.04 ± 0.01	0.13 ± 0.02	40.31 ± 5.1
Soil + NaAc + ZnS (Dark)	7 day	52.22 ± 6.78	2.23 ± 0.07	1.05 ± 0.08	1.09 ± 0.16	0.41 ± 0.07	57.01 ± 5.7
	30 day	32.25 ± 4.15	5.54 ± 0.47	10.15 ± 1.16	0.48 ± 0.12	0.21 ± 0.09	48.64 ± 3.0
	45 day	28.54 ± 2.44	12.97 ± 2.41	5.57 ± 0.78	0.07 ± 0.02	0.23 ± 0.05	47.38 ± 2.9
Soil + NaAc(Dark)	7 day	54.50 ± 5.02	2.92 ± 0.46	1.06 ± 0.06	1.36 ± 0.24	1.27 ± 0.18	61.11 ± 5.9
	30 day	35.60 ± 3.17	8.77 ± 2.01	7.77 ± 0.49	0.07 ± 0.02	0.10 ± 0.02	52.31 ± 2.7
	45 day	29.60 ± 2.87	20.06 ± 3.17	4.65 ± 1.06	0.18 ± 0.07	0.37 ± 0.08	54.86 ± 3.4

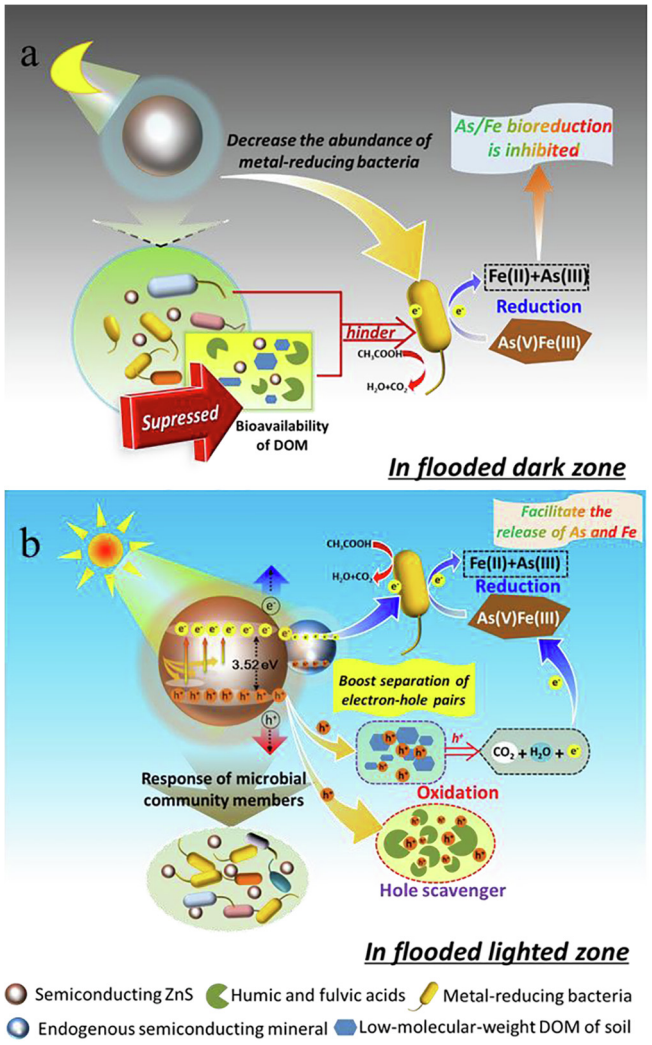

Fig. 7. Mobilization of As and Fe in the ZnS-amended flooded tailing soils under intermittent illumination (a) and dark (b) conditions.

4.4. Role of semiconducting minerals

Knowledge of the potential impacts of semiconducting minerals on metal transformation by sunlight illumination in anoxic arsenic-enrich tailing soils is currently limited. In natural environments, non-photosynthetic microorganisms, semiconducting minerals, DOM, and solar radiation serve as a notable quaternary reciprocal system [7,31,38]. With the presence of semiconducting minerals under illumination, conversion of solar to electrical energy will supply more electrons for As/Fe reduction [11,39]. However, an integrated bioelectro-photocatalytic system can be established when bioavailable electron donors are lacking. This involves the transfer of mineral photoelectrons to metal-reducing bacteria through the minerals, as some minerals have the capacity to serve as electrical conductors [7,51,52]. Photoelectron separation and transfer could alleviate the lack of bio-electrons supplied from microbial degradation of organic matter under extremely adverse conditions. Notably, a variety of semiconducting minerals are present in nature, which may contribute to As/Fe mobilization in tailing soils when they come into contact with indigenous microorganisms [7,53]. Fully assessing the various kinds of minerals (e.g., rutile and pyrite), mobility of metal pollutants, microbial diversity, and bioavailability of DOM in a wide range of soils requires further study. Considering that the environmental impacts might result from interactions among several minerals, research to validate mineral co-occurrence patterns based on a dosage-response protocol is necessary.

This is the first study to report the differential impacts of semiconducting ZnS under illumination and dark conditions on As/Fe mobilization in tailing soils. The mechanisms elucidated in this study influence the fate and transport of metal pollutants by altering their speciation and solubility, and may either weaken or enhance potential environmental risks. Understanding mechanisms resulting from the interactions between microbes, semiconducting minerals, and metal pollutants provide a comprehensive understanding to develop alternative bioremediation technologies. Considering the widespread prevalence of microbes, DOM, and minerals in soils, an alternative solar-microbial extracellular electron transfer pathway is likely to occur in environments where bioavailable electron donors are limited [11,54]. Our work provides a rigorous understanding for the role of semiconducting minerals in the biogeochemical cycling of metals and carbon. Correspondingly, the biogeochemical cycles of metal pollutants and the underlying environmental risk linked to hydrogeological conditions, particularly in sunlight irradiated and anoxic dark zones of flooded soils, deserve further consideration. Overall, these findings have important implications for development of alternative bioremediation strategy for arsenic-polluted soil and for understanding the ecological impact of semiconducting minerals in naturally flooded environments.

5. Conclusions

In this study, we demonstrated the impacts of semiconducting material on As and Fe mobilization in flooded tailing soils. The enhanced reductive dissolution of As(V)/Fe(III) under intermittent illumination was attributed to a microbial-photoelectrochemical synergetic mechanism. In the ZnS treatment with illumination, additional mineral photoelectrons were produced from semiconducting minerals and they subsequently participated in As/Fe reduction, despite a lower

abundance of metal-reducing bacteria. In contrast, under dark conditions, the reductive dissolution of As(V)/Fe(III) was suppressed in ZnS-amended soils due to a decreased abundance of several metal-reducing bacteria (e.g., *Bacillus*, *Geobacter*, *Clostridium*, *Anaeromyxobacter*, and *Desulfitobacterium*). These findings enriched our understanding for the role of semiconducting minerals in the biogeochemical cycle of arsenic-bearing pollutants in flooded tailing soils and inform development of alternative bioremediation strategy for metal-polluted soils.

Acknowledgments

This work was supported by National Natural Science Foundation of China (41807035, 47500101 and 31600401), Project of Research and Development Fund of Wenzhou Medical University (QTJ18034), Natural Science Foundation of Fujian Province of China (2018J05073 and 2018Y0064), Project of Outstanding College Talent of Fujian Province of China (C160091) and Project of Educational Scientific Research of Junior Teacher of Fujian Province of China (JAT170832 and JA13344). We also express our gratitude to Dr. Chih-Hung Wu for fabricating electrochemical reactors in this study.

Appendix A. Supplementary data

Supplementary data to this article can be found online at https://doi.org/10.1016/j.cej.2019.04.130.

References

[1] S. Xue, L. Shi, C. Wu, H. Wu, Y. Qin, W. Pan, W. Hartley, M. Cui, Cadmium, lead, and arsenic contamination in paddy soils of a mining area and their exposure effects on human HEPG2 and keratinocyte cell-lines, Environ. Res. 156 (2017) 23–30.
[2] Z. Chen, H. Li, W. Ma, D. Fu, K. Han, H. Wang, N. He, Q. Li, Y. Wang, Addition of graphene sheets enhances reductive dissolution of arsenic and iron from arsenic contaminated soil, Land. Degrad. Dev. 29 (2018) 572–584.
[3] D. Ociński, I. Jacukowicz-Sobala, P. Mazur, J. Raczyk, E. Kociołek-Balawejder, Water treatment residuals containing iron and manganese oxides for arsenic removal from water – characterization of physicochemical properties and adsorption studies, Chem. Eng. J. 294 (2016) 210–221.
[4] J. Hou, Y. Xiang, D. Zheng, Y. Li, S. Xue, C. Wu, W. Hartley, W. Tan, Morphology-dependent enhancement of arsenite oxidation to arsenate on birnessite-type manganese oxide, Chem. Eng. J. 327 (2017) 235–243.
[5] Z. Chen, Y. Wang, X. Jiang, D. Fu, D. Xia, H. Wang, G. Dong, Q. Li, Dual roles of AQDS as electron shuttles for microbes and dissolved organic matter involved in arsenic and iron mobilization in the arsenic-rich sediment, Sci. Total. Environ. 574 (2017) 1684–1694.
[6] Z. Chen, Y. Wang, D. Xia, X. Jiang, D. Fu, L. Shen, H. Wang, Q. Li, Enhanced bioreduction of iron and arsenic in sediment by biochar amendment influencing microbial community composition and dissolved organic matter content and composition, J. Hazard. Mater. 311 (2016) 20–29.
[7] L. Shi, H. Dong, G. Reguera, H. Beyenal, A. Lu, J. Liu, H.-Q. Yu, J.K. Fredrickson, Extracellular electron transfer mechanisms between microorganisms and minerals, Nat. Rev. Microbiol. 14 (2016) 651–662.
[8] X. Liu, L. Shi, J.-D. Gu, Microbial electrocatalysis: redox mediators responsible for extracellular electron transfer, Biotechnol. Adv. 36 (2018) 1815–1827.
[9] U. Caudillo-Flores, M.J. Muñoz-Batista, F. Ung-Medina, G. Alonso-Núñez, A. Kubacka, J.A. Cortés, M. Fernández-García, Effect of the anatase–rutile contact in gas phase toluene photodegradation quantum efficiency, Chem. Eng. J. 299 (2016) 393–402.
[10] Y. Liu, Q. Li, J. Zhang, W. Sun, S. Gao, J.K. Shang, PdO loaded TiO_2 hollow sphere composite photocatalyst with a high photocatalytic disinfection efficiency on bacteria, Chem. Eng. J. 249 (2014) 63–71.
[11] H.Y. Cheng, X.D. Tian, C.H. Li, S.S. Wang, S.G. Su, H.C. Wang, B. Zhang, H.M.A. Sharif, A.J. Wang, Microbial photoelectrotrophic denitrification as a sustainable and efficient way for reducing nitrate to nitrogen, Environ. Sci. Technol. 51 (2017) 12948–12955.
[12] H. Feng, Y. Liang, K. Guo, N. Li, D. Shen, Y. Cong, Y. Zhou, Y. Wang, M. Wang, Y. Long, Hybridization of photoanode and bioanode to enhance the current production of bioelectrochemical systems, Water Res. 102 (2016) 428–435.
[13] M. Zhao, J. Shi, Z. Zhao, D. Zhou, S. Dong, Enhancing chlorophenol biodegradation: using a co-substrate strategy to resist photo-H_2O_2 stress in a photocatalytic-biological reactor, Chem. Eng. J. 352 (2018) 255–261.
[14] Y. Ma, H. Xiong, Z. Zhao, Y. Yu, D. Zhou, S. Dong, Model-based evaluation of tetracycline hydrochloride removal and mineralization in an intimately coupled photocatalysis and biodegradation reactor, Chem. Eng. J. 351 (2018) 967–975.
[15] W. Tong, Y. Zhang, H. Huang, K. Xiao, S. Yu, Y. Zhou, L. Liu, H. Li, L. Liu, T. Huang, M. Li, Q. Zhang, R. Du, Q. An, A highly sensitive hybridized soft piezophotocatalyst driven by gentle mechanical disturbances in water, Nano Energy 53 (2018) 513–523.
[16] S. Zhang, S. Zhang, L. Song, X. Wu, S. Fang, Synthesis and photocatalytic property of a new silver thiocyanate semiconductor, Chem. Eng. J. 243 (2014) 24–30.
[17] Y. Li, A. Lu, C. Wang, X. Wu, Characterization of natural sphalerite as a novel visible light-driven photocatalyst, Solar Energy Mater. Solar C 92 (2008) 953–959.
[18] L. Zang, C.Y. Liu, X.M. Ren, Photochemistry of semiconductor particles 3. Effects of surface charge on reduction rate of methyl orange photosensitized by ZnS sols, J. Photochem. Photobiol. A 85 (1995) 239–245.
[19] Y. Li, A. Lu, S. Jin, C. Wang, Photo-reductive decolorization of an azo dye by natural sphalerite: case study of a new type of visible light-sensitized photocatalyst, J. Hazard. Mater. 170 (2009) 479–486.
[20] X. Yang, Y. Li, A. Lu, Y. Yan, C. Wang, P.-K. Wong, Photocatalytic reduction of carbon tetrachloride by natural sphalerite under visible light irradiation, Solar Energy Mater. Solar C 95 (2011) 1915–1921.
[21] G. Dong, Y. Huang, Q. Yu, Y. Wang, H. Wang, N. He, Q. Li, Role of nanoparticles in controlling arsenic mobilization from sediments near a realgar tailing, Environ. Sci. Technol. 48 (2014) 7469–7476.
[22] C.H. Wu, S.H. Liu, H.L. Chu, Y.C. Li, C.W. Lin, Feasibility study of electricity generation and organics removal for a molasses wastewater by a waterfall-type microbial fuel cell, J. Taiwan Inst. Chem. E 78 (2017) 150–156.
[23] F. Zhang, J. Liu, I. Ivanov, M.C. Hatzell, W.L. Yang, Y. Ahn, B.E. Logan, Reference and counter electrode positions affect electrochemical characterization of bioanodes in different bioelectrochemical systems, Biotechnol. Bioeng. 111 (2014) 1931–1939.
[24] S.S. Farías, A. Londonio, C. Quintero, R. Befani, M. Soro, P. Smichowski, On-line speciation and quantification of four arsenical species in rice samples collected in Argentina using a HPLC–HG–AFS coupling, Microchem. J. 120 (2015) 34–39.
[25] M. Long, J. Brame, F. Qin, J. Bao, Q. Li, P.J.J. Alvarez, Phosphate changes effect of humic acids on TiO_2 photocatalysis: from inhibition to mitigation of electron–hole recombination, Environ. Sci. Technol. 51 (2017) 514–521.
[26] M.S. Koo, K. Cho, J. Yoon, W. Choi, Photoelectrochemical degradation of organic compounds coupled with molecular hydrogen generation using electrochromic TiO_2 nanotube arrays, Environ. Sci. Technol. 51 (2017) 6590–6598.
[27] H.C. Xu, G.H. Yu, L.Y. Yang, H.L. Jiang, Combination of two-dimensional correlation spectroscopy and parallel factor analysis to characterize the binding of heavy metals with DOM in lake sediments, J. Hazard. Mater. 263 (2013) 412–421.
[28] Y. Liu, S. Wang, L. Zhu, Y. Xia, H. Zhang, S. Wang, X. Yu, J. Lou, F. Li, J. Xu, Pentachlorophenol dissipation and ferrous iron accumulation in flooded paddy soils with contrasting organic matter contents and incorporation of legume green manures, J. Soil Sediment 18 (2018) 2463–2475.
[29] Z. Chu, K. Wang, X. Li, M. Zhu, L. Yang, J. Zhang, Microbial characterization of aggregates within a one-stage nitritation–anammox system using high-throughput amplicon sequencing, Chem. Eng. J. 262 (2015) 41–48.
[30] L. Zhang, X. Yin, S.F.Y. Li, Bio-electrochemical degradation of paracetamol in a microbial fuel cell-Fenton system, Chem. Eng. J. 276 (2015) 185–192.
[31] A.H. Lu, Y. Li, X. Wang, H.R. Ding, C.P. Zeng, X.X. Yang, R.X. Hao, C.Q. Wang, M. Santosh, Photoelectrons from minerals and microbial world: a perspective on life evolution in the early Earth, Precambrian Res. 231 (2013) 401–408.
[32] Z. Chen, G. Dong, L. Gong, Q. Li, Y. Wang, The role of low-molecular-weight organic carbons in facilitating the mobilization and biotransformation of As(V)/Fe(III) from a realgar tailing mine soil, Geomicrobiol. J. 35 (2018) 555–563.
[33] J.Q. Qi, X.C. Li, H. Zheng, P.Q. Li, H.Y. Wang, Simultaneous removal of methylene blue and copper(II) ions by photoelectron catalytic oxidation using stannic oxide modified iron(III) oxide composite electrodes, J. Hazard. Mater. 293 (2015) 105–111.
[34] H. Xiong, S. Dong, J. Zhang, D. Zhou, B.E. Rittmann, Roles of an easily biodegradable co-substrate in enhancing tetracycline treatment in an intimately coupled photocatalytic-biological reactor, Water Res. 136 (2018) 75–83.
[35] J.T. Qiao, X.M. Li, M. Hu, F.B. Li, L.Y. Young, W.M. Sun, W.L. Huang, J.H. Cui, Transcriptional activity of arsenic-reducing bacteria and genes regulated by lactate and biochar during arsenic transformation in flooded paddy soil, Environ. Sci. Technol. 52 (2018) 61–70.
[36] Z. Martín-Moldes, M.T. Zamarro, C. del Cerro, A. Valencia, M.J. Gómez, A. Arcas, Z. Udaondo, J.L. García, J. Nogales, M. Carmona, E. Díaz, Whole-genome analysis of *Azoarcus* sp. strain CIB provides genetic insights to its different lifestyles and predicts novel metabolic features, Syst. Appl. Microbiol. 38 (2015) 462–471.
[37] J.R. Lloyd, D.R. Lovley, Microbial detoxification of metals and radionuclides, Curr. Opin. Biotech. 12 (2001) 248–253.
[38] A.H. Lu, X. Wang, Y. Li, H.R. Ding, C.Q. Wang, C.P. Zeng, R.X. Hao, X.X. Yang, Mineral photoelectrons and their implications for the origin and early evolution of life on Earth, Sci. China Earth Sci. 57 (2014) 897–902.
[39] P. Lianos, Production of electricity and hydrogen by photocatalytic degradation of organic wastes in a photoelectrochemical cell: the concept of the photofuelcell: a review of a re-emerging research field, J. Hazard. Mater. 185 (2011) 575–590.
[40] A.H. Lu, Y. Li, S. Jin, X. Wang, X.L. Wu, C.P. Zeng, Y. Li, H.R. Ding, R.X. Hao, M. Lv, C.Q. Wang, Y.Q. Tang, H.L. Dong, Growth of non-phototrophic microorganisms using solar energy through mineral photocatalysis, Nat. Commun. 3 (2012) 1–8.
[41] K.L. Bae, J. Kim, C.K. Lim, K.M. Nam, H. Song, Colloidal zinc oxide-copper(I) oxide nanocatalysts for selective aqueous photocatalytic carbon dioxide conversion into methane, Nat. Commun. 8 (2017) 1–8.
[42] A.M. Hansen, T.E.C. Kraus, B.A. Pellerin, J.A. Fleck, B.D. Downing, B.A. Bergamaschi, Optical properties of dissolved organic matter (DOM): effects of biological and photolytic degradation, Limnol. Oceanogr. 61 (2016) 1015–1032.
[43] M. Gmurek, M. Olak-Kucharczyk, S. Ledakowicz, Photochemical decomposition of endocrine disrupting compounds – a review, Chem. Eng. J. 310 (2017) 437–456.
[44] J. Yan, G. Wu, N. Guan, L. Li, Z. Li, X. Cao, Understanding the effect of surface/bulk

defects on the photocatalytic activity of TiO_2: anatase versus rutile, Phys. Chem. Chem. Phys. 15 (2013) 10978–10988.
[45] L. Zhang, Q. Zheng, Y. Xie, Z. Lan, O.V. Prezhdo, W.A. Saidi, J. Zhao, Delocalized impurity phonon induced electron–hole recombination in doped semiconductors, Nano Lett. 18 (2018) 1592–1599.
[46] H.J. Kim, J.H. Kim, I.K. Durga, D. Punnoose, N. Kundakarla, A.E. Reddy, S.S. Rao, Densely packed zinc sulfide nanoparticles on TiO_2 for hindering electron recombination in dye-sensitized solar cells, New J. Chem. 40 (2016) 9176–9186.
[47] V. Chakrapani, D. Baker, P.V. Kamat, Understanding the role of the sulfide redox couple (S^{2-}/S_n^{2-}) in quantum dot-sensitized solar cells, J. Am. Chem. Soc. 133 (2011) 9607–9615.
[48] D.J. Richardson, J.N. Butt, J.K. Fredrickson, J.M. Zachara, L. Shi, M.J. Edwards, G. White, N. Baiden, A.J. Gates, S.J. Marritt, T.A. Clarke, The 'porin-cytochrome' model for microbe-to-mineral electron transfer, Mol. Microbiol. 85 (2012) 201–212.
[49] X.Y. Xiao, J. Jiang, L.Z. Zhang, Selective oxidation of benzyl alcohol into benzaldehyde over semiconductors under visible light: the case of $Bi_{12}O_{17}Cl_2$ nanobelts, Appl. Catal. B-environ. 142 (2013) 487–493.
[50] X.Z. Li, F.B. Li, C.M. Fan, Y.P. Sun, Photoelectrocatalytic degradation of humic acid in aqueous solution using a Ti/TiO_2 mesh photoelectrode, Water Res. 36 (2002) 2215–2224.
[51] Z.Q. Lin, S.J. Yuan, W.W. Li, J.J. Chen, G.P. Sheng, H.Q. Yu, Denitrification in an integrated bioelectro-photocatalytic system, Water Res. 109 (2017) 88–93.
[52] J.M. Byrne, N. Klueglein, C. Pearce, K.M. Rosso, E. Appel, A. Kappler, Redox cycling of Fe(II) and Fe(III) in magnetite by Fe-metabolizing bacteria, Science 347 (2015) 1473.
[53] S.G. Zhou, J.H. Tang, Y. Yuan, G.Q. Yang, B.S. Xing, TiO_2 nanoparticle-induced nanowire formation facilitates extracellular electron transfer, Environ. Sci. Technol. Lett. 5 (2018) 564–570.
[54] J.M. Pisciotta, Y.J. Zou, I.V. Baskakov, Role of the photosynthetic electron transfer chain in electrogenic activity of cyanobacteria, Appl. Microbiol. Biotechnol. 91 (2011) 377–385.